·专题论著·

刘彤，医学博士/博士后（美国Cedars-Sinai医学中心），主任医师，教授，博士研究生导师，天津医科大学第二医院心脏科科长，天津医科大学科技处副处长，天津心脏病学研究所副所长。入选国家百千万人才工程，中华人民共和国人力资源和社会保障部有突出贡献中青年专家，天津市131创新型人才（第一层次），首批天津市津门医学英才。主要从事心脏起搏与射频消融、心房颤动的基础和临床研究，肿瘤心脏病学的基础与临床研究。现任国家卫生健康委人才交流服务中心心律失常诊疗高级人才能力建设项目专家委员会副主任委员，中国医疗保健国际交流促进会心律与心电分会第三届委员会副主任委员，中华医学会心脏起搏与电生理分会委员，中华医学会心血管病分会青年委员，国际心电学会青年委员，欧洲心脏学会专家会员，中国抗癌协会整合肿瘤心脏病学分会常务委员，《中国心血管病研究杂志》青年编委会主任委员，《中华心律失常学杂志》通讯编委。承担国家自然科学基金项目5项，京津冀基础合作专项1项，天津市科技局重点项目2项，获天津市科技进步奖3项，在*Journal of the American College of Cardiology*、*JAMA Internal Medicine*、*Redox Biology*、*Stroke*、*Circulation: Arrhythmia and Electrophysiology*等SCI收录期刊上以第一作者及通信作者发表文章100余篇，H指数为33，总引用次数6 342次，主编及主译专著5部，副主编及副主译专著7部。

阿霉素诱导心肌病小鼠模型的构建

张庆领，张云鹏，周赞东，张　跃，刘　彤

天津医科大学第二医院心脏科，天津市心血管病离子与分子机能重点实验室，天津心脏病学研究所，天津 300211

［**摘要**］ **背景与目的：**阿霉素又称多柔比星，是临床实践中治疗各种肿瘤中有效、应用广泛的细胞毒性化疗药物之一，属于蒽环类抗肿瘤药物。然而该药物会引起严重的不良反应，特别是剂量依赖性心脏毒性，因而成为肿瘤心脏病学领域颇受关注的问题。目前国际上尚无公认、统一、稳健的阿霉素诱导心肌病模型的构建方法。为探讨最佳给药剂量及频次构建阿霉素诱导急性心肌病设计本实验。**方法：**40只8～10周龄雄性C57BL/6J小鼠随机分为4组：对照组（control，CON）给予等量生理盐水腹腔注射，以及在阿霉素累积剂量相同的情况下，根据不同给药剂量及频次的M1组（单次给药15 mg/kg）、M2组（单次5 mg/kg，连续3d给药）、M3组（单次7.5 mg/kg，隔天给药，共2次）腹腔注射阿霉素构建阿霉素诱导急性心肌病模型。分别从小鼠一般生命体征、体重变化和存活率、心脏超声、体表心电图、N末端B型利钠肽原（N-terminal pro-B-type natriuretic peptide，NT-proBNP）、心肌肌钙蛋白I（cardiac troponin I，cTnI）及心肌组织形态改变等方面综合评估造模效果。**结果：**与CON相比，M1、M2、M3组小鼠体重均显著下降（$P<0.001$）；M3组较M1和M2组存活率更高（80% *vs* 40%、50%，$P<0.05$）。相较于CON、M1组和M2组，体表心电图显示M3组PR间期［（0.064 2±0.003 8）s *vs*（0.042 3±0.000 9）s、（0.052 7±0.007 9）s和（0.062 0±0.001 2）s，P均<0.05］、QT间期［（0.047 5±0.000 2）s *vs*（0.022 0±0.000 9）s、（0.038 6±0.004 4）s和（0.044 4±0.003 0）s，P均<0.05］显著延长；心脏超声检查结果显示，M3左心室射血分数显著下降（40.40%±2.24% *vs* 54.72%±1.64%、46.00%±4.41%和54.68%±3.38%，P均<0.05），M3左心室短轴缩短率显著下降（19.40%±1.20% *vs* 27.88%±1.05%、22.57%±2.50%和27.86%±2.20%），差异有统计学

基金项目：天津市研究生科研创新项目（2021YJSB278），国家自然科学基金（81970270、82170327），天津市医学重点学科（专科）建设项目（TJYXZDXK-029A）。

第一作者：张庆领（ORCID：0000-0002-0323-0042），E-mail: zhangqingling2020@tmu.edu.cn。
通信作者：刘　彤（ORCID：0000-0003-0482-0738），E-mail: liutongdoc@126.com。

意义（*P*均＜0.05）；心脏标志物检测显示，与CON相比，阿霉素给药组M1组、M2组、M3组血清NT-proBNP水平显著升高［（638.13±12.69）pg/mL *vs*（1 271.36±11.76）pg/mL、（1 270.85±36.19）pg/mL和（1 225.26±24.19）pg/mL，*P*均＜0.05）。组织形态学显示，M3心肌细胞空泡化程度及数量显著高于CON、M1和M2（81个/视野 *vs* 3个/视野、65个/视野、34个/视野，*P*＜0.05）。**结论：**腹腔注射阿霉素诱导急性心肌病模型的方法简便、可靠；阿霉素腹腔注射剂量7.5 mg/kg，隔天给药2次，累积剂量15 mg/kg模型最理想。

［**关键词**］ 阿霉素心脏毒性；心肌病；肿瘤心脏病；模型

DOI: 10.19401/j.cnki.1007-3639.2022.10.003

中图分类号：R542.2 **文献标志码：**A **文章编号：**1007-3639(2022)10-0948-12

Construction of a mouse model of adriamycin-induced cardiomyopathy

ZHANG Qingling, ZHANG Yunpeng, ZHOU Zandong, ZHANG Yue, LIU Tong (Tianjin Key Laboratory of Ionic-Molecular Function of Cardiovascular Disease, Department of Cardiology, Tianjin Institute of Cardiology, the Second Hospital of Tianjin Medical University, Tianjin 300211, China)

Correspondence to: LIU Tong, E-mail: liutongdoc@126.com.

［**Abstract**］**Background and purpose:** Adriamycin also named as doxorubicin, is one of the most widely used cytotoxic chemotherapeutic agents for clinical practice for the treatment of various tumors, and belongs to anthracycline antitumor drugs. Unfortunately, this drug will cause serious side effects, especially dose-dependent cardiotoxicity, which has become a concern in the field of onco-cardiology. At present, there is no universally recognized, unified and robust method to construct Doxorubicin-induced cardiomyopathy model. This experiment was designed to explore the optimal dose and frequency of doxorubicin-induced cardiomyopathy in a mouse model. **Methods:** Forty 8-10-week-old male C57BL/6J mice were randomly divided into 4 groups (control group and 3 model groups). The model group was divided into model 1 (M1) group (15 mg/kg, single dose) and M2 group (5 mg/kg, once a day for 3 days continuously) and M3 group (7.5 mg/kg, twice on alternate days). General vital signs (body weight change and survival rate), echocardiography, body surface electrocardiogram (ECG), N-terminal pro-B-type natriuretic peptide (NT-proBNP), cardiac troponin I (cTnI) and myocardial tissue morphological changes were evaluated comprehensively. **Results:** Compared with the control group, the body weight of mice in M1, M2 and M3 groups decreased significantly (*P*＜0.001); M3 group had higher survival rate than M1 and M2 group (80% *vs* 40% and 50%, *P*＜0.05). Compared with the control group, M1 group and M2 group, the body surface ECG showed that the PR interval of M3 group ［(0.064 2±0.003 8)s *vs* (0.042 3±0.000 9)s, (0.052 7±0.007 9)s and (0.062 0±0.001 2)s, *P*＜0.05］ and QT interval ［(0.047 5±0.000 2)s *vs* (0.022 0±0.000 9)s, (0.038 6±0.004 4)s and (0.044 4±0.003 0)s, *P*＜0.05］ were significantly prolonged. Cardiac ultrasound showed that M3 ejection fraction decreased significantly (40.40%±2.24% *vs* 54.72%±1.64%, 46.00%±4.41% and 54.68%±3.38%, *P*＜0.05). M3 short-axis shortening rate decreased significantly (19.40%±1.20% *vs* 27.88%±1.05%, 22.57%±2.50% and 27.86%±2.20%, *P*＜0.05). Cardiac markers showed that compared with CON , the serum NT-proBNP levels of M1 , M2 and M3 in adriamycin group were significantly increased ［(638.13±12.69) pg/mL *vs* (1 271.36±11.76) pg/mL, (1 270.85±36.19) pg/mL and (1 225.26±24.19) pg/mL, *P*＜0.05］. Histomorphology showed that the vacuoles in cardiomyocyte of M3 group was significantly increased compared with CON, M1 and M2 group (81/field *vs* 3/field, 65/field and 34/field, *P*＜0.05). **Conclusion:** Intraperitoneal injection of adriamycin in acute heart failure model is simple and reliable. The model in which adriamycin is administered by intraperitoneal injection at a dose of 7.5 mg/kg, twice on alternate days, with cumulative dose of 15 mg/kg is optimal.

［**Key words**］Adriamycin-induced cardiotoxicity; Cardiomyopathy; Onco-cardiology; Model

随着医疗技术的进步，全球癌症患者生存率显著提高[1]。美国的癌症患者平均5年生存率是66%[2]；国家癌症中心2022年数据显示，中国过去10余年恶性肿瘤生存率呈逐渐上升趋势，目前中国恶性肿瘤患者的5年相对生存率约为40.5%[3]。然而，在肿瘤幸存者中心血管疾病的发生率和死亡率仅次于肿瘤复发，乳腺癌患者10年后因心脏疾病所致死亡的风险已超过肿瘤本身[4]；儿童肿瘤患者治疗后，其因心脏病死亡发生风险为正常人的8倍[5]；青年肿瘤幸存者心血管发病风险增加20倍[6]。因此，如何降低肿瘤治疗伴随的心脏毒性是临床实践中亟待解决、备受关注的关键问题之一。

在现行诸多肿瘤化疗方案中，阿霉素

（adriamycin）又称多柔比星（doxorubicin），是临床较常用的化疗药物之一[7-10]。阿霉素是从波赛链真菌变种链真菌发酵液中提取的一种糖苷类抗生素，既可抑制RNA合成，也可阻止DNA复制，属于细胞周期非特异性药物[11]，在临床上广泛应用于各种恶性肿瘤的治疗[12]。药物代谢动力学研究发现阿霉素细胞毒性主要与“血药浓度-时间”曲线下面积相关，但其急性心脏毒性主要与峰浓度相关[13]。由阿霉素毒性引起的心肌损伤，即阿霉素诱导的心肌病严重影响患者的生活质量和幸存时间。阿霉素诱导的心肌病的发病机制及治疗策略是研究者关注的主要方向，然而已发表的文献对阿霉素诱导的心肌病模型构建的给药累积剂量、给药频次、造模周期各不相同，目前国际上尚无公认、统一、稳健的阿霉素诱导的心肌病模型构建方法。本研究通过临床患者常用阿霉素化疗方案用药累积剂量等量换算为小鼠用药剂量，设置相同累积剂量下不同给药周期，研究比较各组小鼠一般情况、血流动力学、心电生理检查、超声心动图、心肌组织形态学等指标的病理生理学改变；综合分析选择最佳阿霉素诱导的心肌病小鼠模型，为未来研究阿霉素诱导的心肌病发病机制及干预策略、提高动物福利、减少实验成本等提供理论支持。

1 材料和方法

1.1 实验动物及模型构建分组

40只8~10周龄雄性C57BL/6J小鼠，由北京维通利华实验动物技术有限公司提供。饲养环境温度保持在（23±2）℃，自然光暗周期为12 h/12 h，鼠笼垫料隔天更换1次。

根据欧洲肿瘤内科学会（European Society for Medical Oncology，ESMO）指南[14]推荐，蒽环类药物的最大累积剂量限制为450 ~ 550 mg/m^2，本研究按推荐的最大累积剂量取550 mg/m^2；根据体表面积（body surface area，BSA）公式计算成年人（60 kg/170 cm）体表面积。通过计算得出最大累积剂量为15.125 mg/kg。因此，我们在后面文章中使用了最大累积剂量为15 mg/kg进行造模。

实验动物分别编号并随机分组，分为4组：① 对照组（Control, CON），为等剂量生理盐水腹腔注射（n=10）；② 阿霉素（D107159，上海阿拉丁生化科技股份有限公司）模型组1（model 1，M1），单次给药15 mg/kg腹腔注射，总剂量为15 mg/kg（n=10）[15]；③ 阿霉素模型组2（model 2，M2），单次5 mg/kg腹腔注射，连续3d给药，总剂量为15 mg/kg（n=10）；④ 模型组3（model 3，M3），单次7.5 mg/kg腹腔注射，隔天给药，共2次，总剂量为15 mg/kg（n=10）[16]；所有模型组动物均于最后1次给药1周后处死。本研究经天津医科大学伦理委员会批准同意，实验操作符合3R原则。

1.2 小鼠一般情况观察

造模前分别进行小鼠基线体重测量。造模后每天测量小鼠体重；同时观察小鼠的精神状态、进食情况、毛发、日常活动情况、排便情况，同时记录各组小鼠存活情况。

1.3 小鼠超声心动图

留取小鼠胸骨旁左心室长轴、短轴切面B型和M型模式标准图像，测量室间隔厚度、左心室后壁厚度、左心室收缩末期直径及左心室舒张末直径。左心室射血分数（left ventricular ejection fraction，LVEF）及左心室短轴缩短率（left ventricular fractional shortening，LVFS）由M型超声图像测量得出。

1.4 电生理学实验

5%的戊巴比妥钠腹腔麻醉满意后，连接小鼠肢体导联，描记体表心电图。之后给予气管插管，小动物呼吸机辅助呼吸；经胸骨正中切口小心快速开胸，充分暴露心脏，使用EMapScope 3.0操作系统进行数据记录，将多电极阵列标测系统置于右心室外膜进行右室传导电标测描记。同样的方法进行左心室电生理标测。通过分析体表心电图及Mapping数据评估阿霉素对心脏传导系统的影响。

1.5 组织学

取小鼠心脏组织，用4%中性甲醛溶液固定，用石蜡包埋24 h。然后将包埋的组织切成5

μm切片。切片用H-E染色，光镜检查。通过H-E染色，观察细胞形态，评估阿霉素诱导心肌细胞损伤情况。通过Masson染色观察心肌胶原纤维。经过核染、浆染、分色、复染等步骤，心肌组织中纤维成分被染为蓝色，正常的心肌组织为红色。通过计算胶原纤维分数［蓝色面积/（蓝色面积＋红色面积）×100%］评估心肌纤维化程度。H-E染色和Masson染色均为每张玻片取40倍物镜视野下随机拍摄5张照片。应用Image J处理图像，分别计算每个视野下胶原纤维分数，并进行统计学分析。

1.6 酶联免疫吸附试验（enzyme-linked immunosorbent assay，ELISA）法检测

采用ELISA法检测血清心肌肌钙蛋白I（cardiac troponin I，cTnI）、N末端B型利钠肽原（N-terminal pro-B-type natriuretic peptide，NT-proBNP）。所有小鼠于最后1次阿霉素给药1周后进行心脏取血。应用肝素抗凝，经高速离心机10 000 r/min，在4 ℃下离心5 min。分离上清液150～300 μL存储于−80 ℃深低温冰箱。于24 h内应用ELISA试剂盒检测小鼠血清中的心脏标志物NT-proBNP、cTnI水平。

1.7 统计学处理

采用Fiji软件处理图像，采用SPSS 26.0软件进行统计学分析，采用GraphPad Prism 8软件制作统计图表。所有实验数据以$\bar{x}\pm s$表示，多组间比较采用Bonferroni校正后的单因素方差分析（one-way ANOVA）进行统计分析。$P<0.05$为差异有统计学意义。

2 结　果

2.1 现有文献关于小鼠阿霉素诱导的心肌病造模方式的总结

我们在“Web of Science 核心合集”数据库中分别使用检索式1“adriamycin （主题）AND cardiotoxicity（主题）AND 2018—2022（出版年）”和检索式2“doxorubicin（主题）AND cardiotoxicity（主题）AND 2018—2022（出版年）”检索最近5年数据资料，共检索有关阿霉素（多柔比星）心脏毒性的研究2 732篇（其中检索1包含228篇，检索式2包含2 504篇）文章。排除综述类文章446篇（检索式1包含39篇，检索式2包含407篇）。在剩余的2 286篇中，我们筛选高被引用文献20篇纳入统计。排除非小鼠模型7篇，最终纳入13篇文献（表1）。

表1 阿霉素小鼠模型造模总结

Tab. 1 Summary of doxorubicin mouse model in document literature

Reference	Cumulative dose	Mode of administration
［17］	7 mg	1 mg/kg, once a day for continued 7 days
［15, 18］	15 mg	15 mg/kg, once
［19］		2.5 mg/kg, every other day, six times in a row
［15］		5 mg /kg, once a week for 3 weeks
［16］		7.5 mg/kg, twice on alternate days
［20］	16 mg	4 mg/kg, once a week for 4 weeks
［21］	18 mg	6 mg/kg, via tail vein at day 0, 2, and 4
［22-23］	20 mg	5 mg/kg, once a week for 4 weeks
［24］		20 mg/kg, once
［25］	24 mg	6 mg/kg, once a week for 4 weeks
［26-27］	25 mg	5 mg/kg, once a week for 5 weeks

2.2 一般情况改变

实验分组如图1A所示。实验结束后，使用实验结束时的终体重占基线体重的百分率评价阿霉素对小鼠体重的影响。实验结果显示，相较CON（105.96%±0.92%），M1组（84.36%±5.40%）、M2组（92.58%± 2.26%）和M3组（85.25%±2.17%）体重显著下降（图1B）。给予阿霉素后，小鼠一般情况恶化，包括进食差，精神状态欠佳、萎靡，活动强度减弱，逐渐出现死亡动物等。M1、M2在给药后第3天小鼠开始出现死亡，至造模结束时，M1小鼠死亡率为60%，M2死亡率为50%，M3死亡率为20%（图1C）。

2.3 心电生理改变

各组间体表心电图描记见图2A。相较

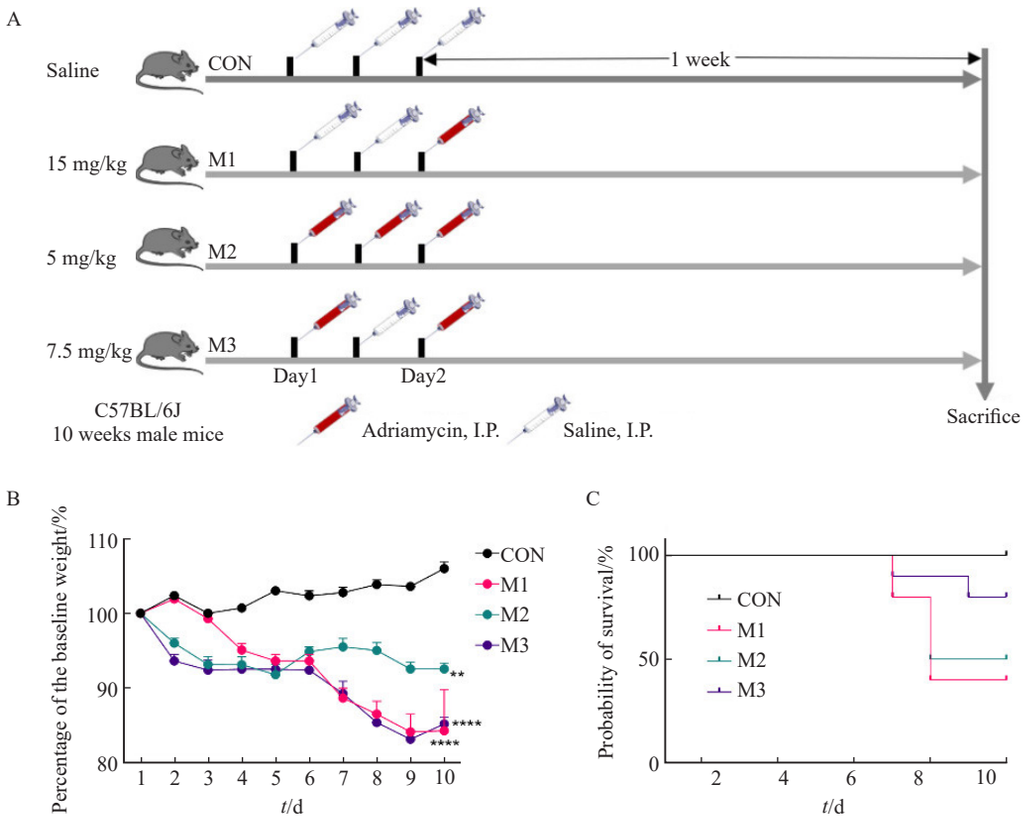

图1 小鼠一般情况监测

Fig. 1 Mice general condition monitoring

A: Grouping and treatment; B: Change trend of percentage of body weight relative to baseline body weight in control group and model group; C: Survival curves of mice in control group and model group. CON: Control group; M1: Model group 1; M2: Model group 2; M3: Model group 3; **: P<0.01, compared with each other; ****: P<0.000 1, compared with each other; Data were expressed as $\bar{x}\pm s$.

于CON、M1和M2，体表心电图检测结果显示，M3的PR间期［（0.064 2±0.003 8）s *vs*（0.042 3±0.000 9）s、（0.052 7±0.007 9）s、（0.062 0±0.001 2）s，P均<0.05，图2B和表2］、QT间期［（0.047 5±0.000 2）s *vs*（0.022 0±0.000 9）s、（0.038 6±0.004 4）s、（0.044 4±0.003 0）s，P均<0.05，图2C］及QTc间期［（0.637 7±0.004 2）s *vs*（0.148 5±0.008 6）s、（0.152 2±0.007 6）s、（0.143 3±0.011 7）s］时限显著延长（表2）；P波时限［（0.015 3±0.001 2）s *vs*（0.014 0±0.001 3）s、（0.012 0±0.000 7）s、（0.012 1±0.000 3）s，P均>0.1］、QRS时限［（0.010 3±0.000 6）s *vs*（0.011 2±0.001 0）s、（0.010 5±0.000 8）s、（0.010 5±0.000 1）s，P均>0.1］、RR间期［（0.164 8±0.017 5）s *vs*（0.148 5±0.008 6）s、（0.152 2±0.007 6）s、（0.143 3±0.011 7）s，P均>0.1，表2］差异无统计学意义。

在体心外膜电传导（mapping）结果如图所示（图3A）。与CON相比，模型组传导速度显著下降［（0.89±0.12） mm/ms *vs*（0.59±0.05）mm/ms、（0.28±0.07）mm/ms、（0.55±0.10）mm/ms，P均<0.05，图3B］，传导异质性增加［（2.01±0.16）ms/mm *vs*（4.43±0.35）ms/mm、（3.99±0.20）ms/mm、（3.29±0.22）ms/mm，P均<0.05，图3C］；异质性指数差异无统计学意义（图3D）。

2.4 心功能改变

各组小鼠超声心动图结果见图4A。M3的LVEF较CON、M1和M2组，显著下降（40.40%±2.24% *vs* 54.72%±1.64%、46.00%±4.41%和54.68%±3.38%，图4B）。

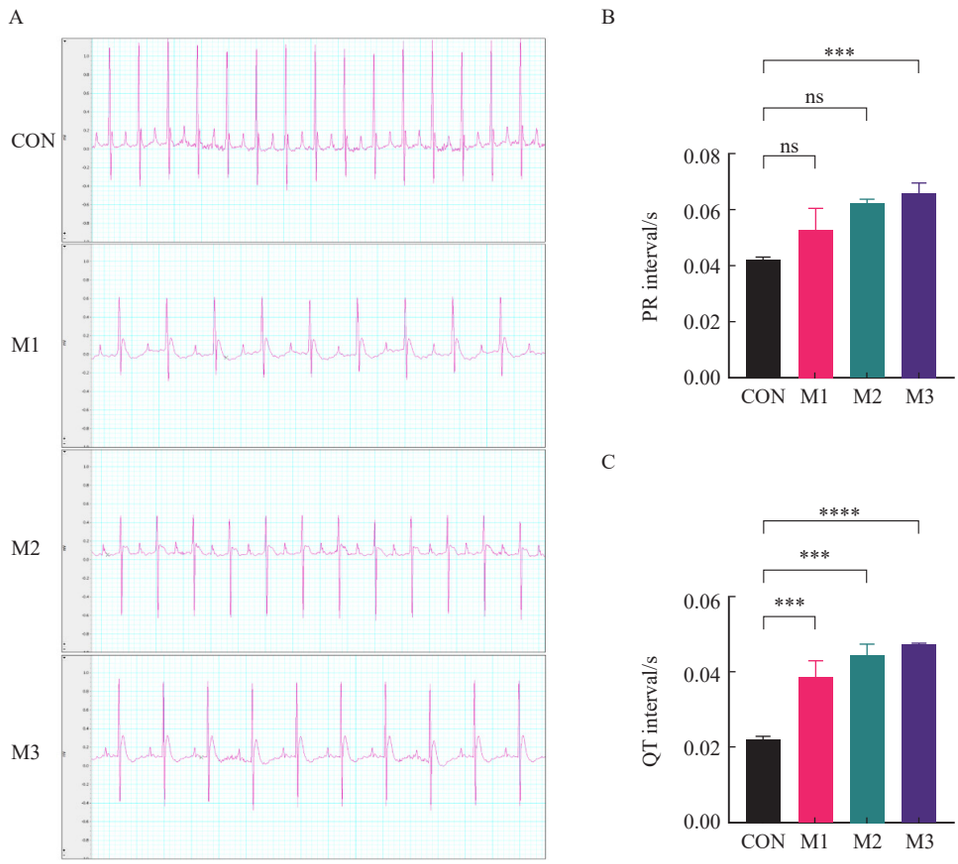

图2 各组小鼠体表心电图和统计结果

Fig. 2 Electrocardiogram and statistical results of each group

A: Typical electrocardiogram; Arrows showed: T-wave flattening and duration extension in each model group; B-C: Statistical results of PR interval and QT interval; CON: Control group; M1: Model group 1; M2: Model group 2; M3: Model group 3; ***: P<0.001, compared with each other; ****: P<0.000 1, compared with each other; Data were expressed as $\bar{x}\pm s$. ns: No statistical significance.

表2 各组小鼠心脏超声和体表心电图参数比较

Tab. 2 Comparison of echocardiography and electrocardiogram parameters in each group

Item	CON	M1	M2	M3
$LVID^d$/mm	3.752 4±0.133 9	3.738 9±0.152 0	3.427 8±0.157 4	3.247 3±0.229 8
$LVID^s$/mm	2.706 6±0.104 7	2.707 0±0.142 0	2.470 1±0.124 2	2.486 2±0.180 3
$LVPW^d$/mm	0. 715 0±0.045 7	0.639 3±0.056 6	0.710 2±0.013 1	0.717 2±0.048 3
$LVPW^s$/mm	0.990 9±0.027 5	0.686 3±0.019 6	0.916 1±0.030 3	0.927 0±0.071 7
IVS^d/mm	0.787 2±0.075 6	0.822 8±0.100 7	0.778 2±0.049 9	0.727 3±0.053 9
IVS^s/mm	1.200 4±0.039 3	1.130 3±0.182 4	0.951 7±0.027 9	0.940 5±0.046 2
LVEF/%	54.722 9±1.635 1	46.009 3±4.413 7	54.684 3±3.375 4	40.396 6±2.240 7*
LVFS/%	27.880 8±1.050 3	22.568 3±2.503 1	27.857 9±2.202 7	19.395 5±1.207 5*
P wave duration/s	0.014 0±0.001 3	0.012 0±0.000 7	0.012 1±0.000 3	0.015 3±0.001 2
PR interval/s	0.042 3±0.000 9	0.052 7±0.007 9	0.062 0±0.001 2	0.064 2±0.003 8**
QRS duration/s	0.011 2±0.001 0	0.010 5±0.000 8	0.010 5±0.000 1	0.010 3±0.000 6

续表2 各组小鼠心脏超声和体表心电图参数比较

Item	CON	M1	M2	M3
QT interval/s	0.022 0±0.000 9	0.038 6±0.004 4*	0.044 4±0.003 0**	0.047 5±0.000 2**
QTc interval/s	0.041 9±0.002 0	0.072 1±0.007 5*	0.848 1±0.003 4**	0.637 7±0.004 2*
RR interval/s	0.148 5±0.008 6	0.152 2±0.007 6	0.143 3±0.011 7	0.164 8±0.017 5

LVID: Left ventricular diameter; LVPW: Left ventricular posterior wall thickness; IVS: Thickness of ventricular septum; LVEF: Left ventricular ejection fraction; LVFS: Left ventricular shortening fraction. d: Diastolic; s: Systolic; *: $P<0.01$, compared with CON group; **: $P<0.000\ 1$, compared with CON group.

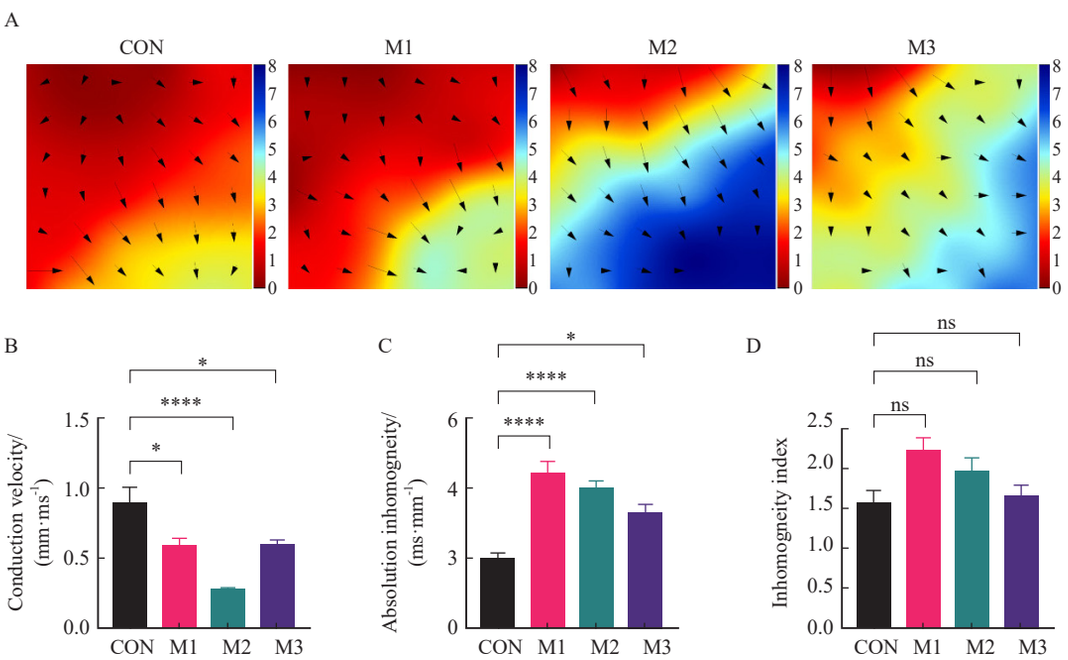

图3 各组小鼠心室心外膜电传导图像和统计结果

Fig. 3 Ventricular epicardial electrical conduction images and statistical results of mice in each group

A: Mapping diagram; B-D: Mapping statistical results; CON: Control group; M1: Model group 1; M2: Model group 2; M3: Model group 3; *: $P<0.05$, compared with each other; ****: $P<0.000\ 1$, compared with each other; Data were expressed as $\bar{x}\pm s$. ns: No statistical significance.

此外，M3左心室短轴缩短率与CON、M1、M2相比显著下降（19.40%±1.20% *vs* 27.88%±1.05%、22.57%±2.50%和27.86%±2.20%，图4C）。胸骨旁左心室长轴和短轴切面显示，IVS、LVPW、LVID在收缩和舒张期差异无统计学意义（表2）。

2.5 阿霉素给药组血清NT–proBNP显著升高

临床上常应用心脏标志物来评估心肌损伤和心功能恶化程度，如CK和CK-MB、cTnI、BNP、NT-proBNP、MPO等。本研究选用了临床上较常使用的血清NT-proBNP、cTnI用以评估阿霉素心肌病模型中实验对象心功能和心肌损伤水平[28]。阿霉素各给药组血清NT-proBNP水平［M1组（1 271.36±11.76）pg/mL、M2组为（1 270.85±36.19）pg/mL，M3组为（1 225.26±24.19）pg/mL］较CON［（638.13±12.69）pg/mL］显著升高（P均<0.05，图5A），提示阿霉素给药后实验动物模型出现了心力衰竭。

各阿霉素给药组血清cTnI水平［M1组为（41.24±2.39）ng/L、M2组为（40.84±2.12） ng/L、M3组为（47.04±6.60）ng/L］与CON［（38.85±1.14）ng/L］相比，差异无统计学意义（P均>0.05，图5B）。

2.6 心肌组织形态学改变

既往研究[29]表明，阿霉素所致心肌细胞损

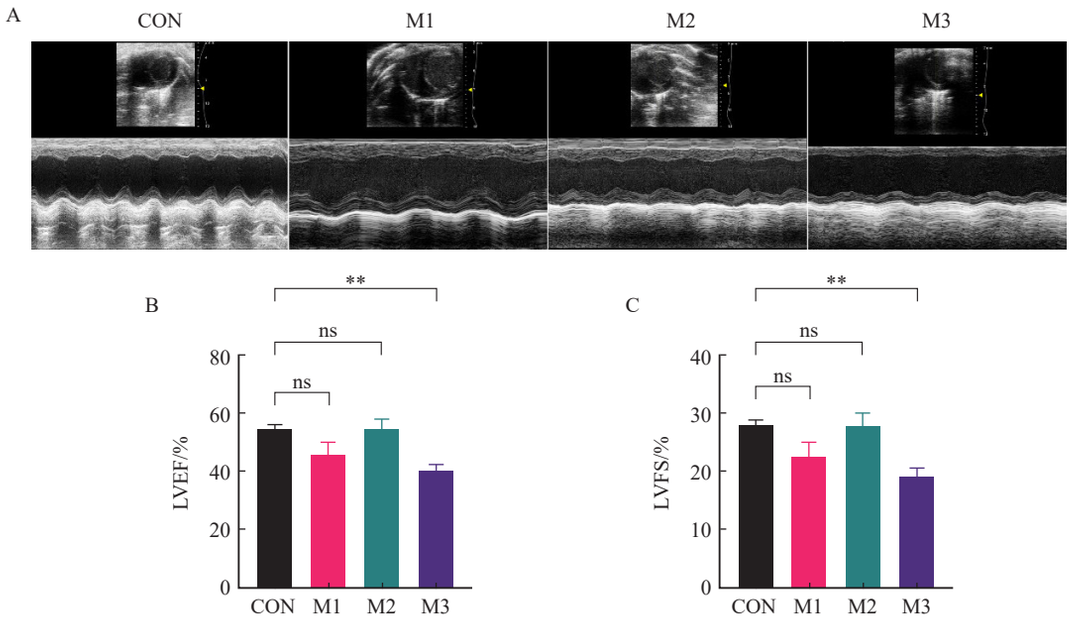

图4 各组小鼠胸骨旁左心室短轴切面M型超声图像和统计结果

Fig. 4 M-model ultrasound images and statistical results of parasternal left ventricle in short axis section of mice in each group

A: M-model ultrasound images of parasternal left ventricle in short axis section in each group; B-C: The statistical results of LVEF and LVFS; CON: Control group; M1: Model group 1; M2: Model group 2; M3: Model group 3; **: P<0.01, compared with each other; Data were expressed as $\bar{x}\pm s$. ns: No statistical significance.

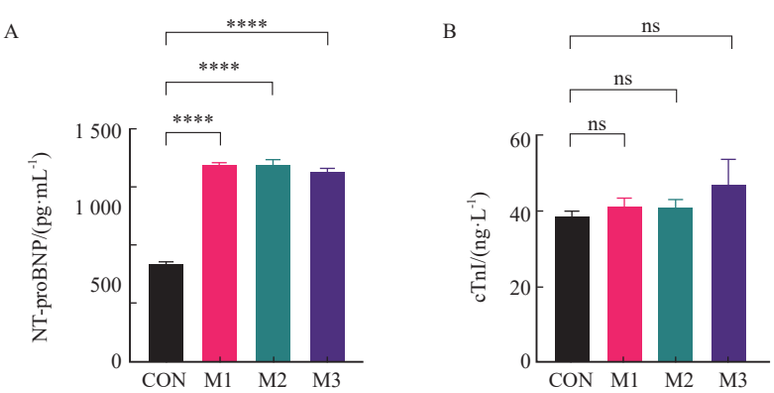

图5 血清NT–proBNP、cTnI检测结果

Fig. 5 The levels of Serum NT-proBNP and cTnI

A: NT-proBNP; B: NT-proBNP; CON: Control group; M1: Model group 1; M2: Model group 2; M3: Model group 3; ****: P<0.000 1, compared with each other; Data were expressed as $\bar{x}\pm s$. ns: No statistical significance.

伤，在细胞水平上表现为心肌细胞胞浆空泡化、肌原纤维紊乱和丢失。本实验中动物心肌组织H-E染色结果见图6。与CON相比，模型组心肌均可见心肌细胞空泡化变性，细胞径向增大（图6B），部分肌纤维走向紊乱；其中M3心肌细胞空泡化程度及数量显著高于CON、M1和M2（81个/视野 *vs* 3个/视野、65个/视野、34个/视野，P＜0.05），细胞径向增大最明显（图6B）。与M1相比，M2、M3中阿霉素所致的心肌细胞空泡化数量减少，心肌细胞纤维排列紊乱较轻。Masson染色未见心肌纤维显著的纤维化改变，纤维化面积各组之间差异无统计学意义（图6A、C），考虑可能与造模时间较短有关。

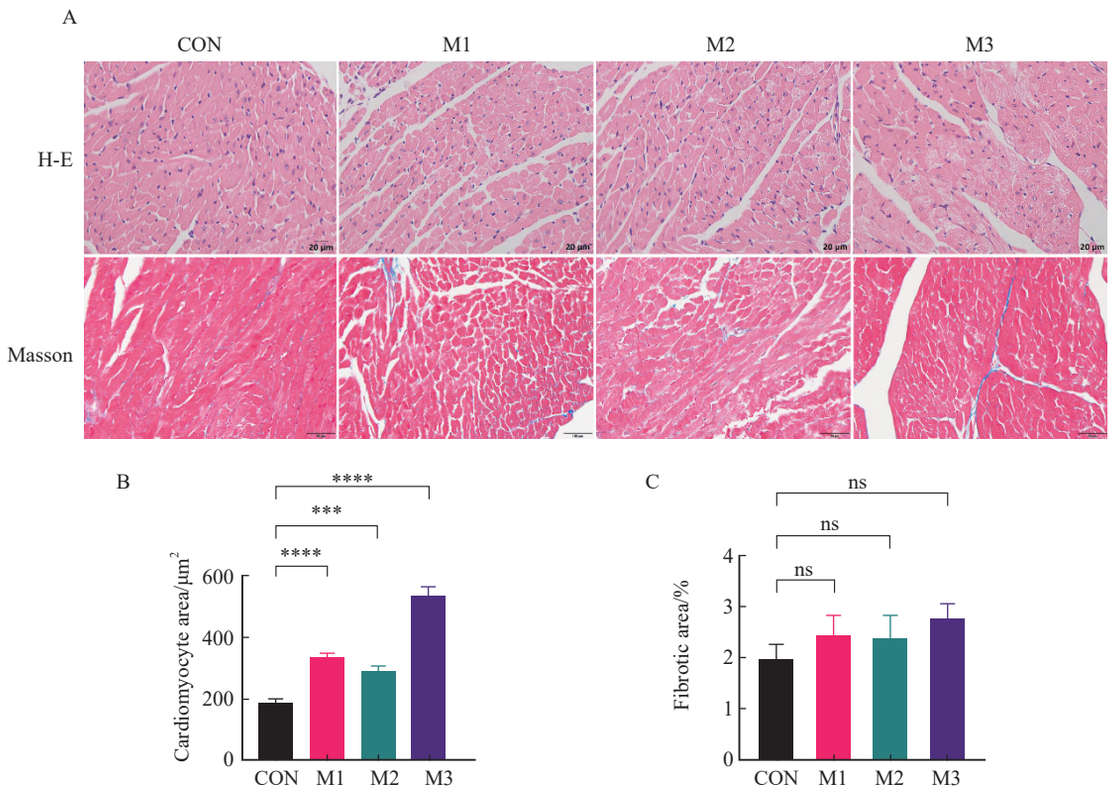

图6 各组心室组织H-E染色及Masson染色结果

Fig. 6 H-E staining and Masson staining of left ventricular tissue in each group

A: H-E staining and Masson staining; B: Cardiomyocyte vacuoles number; C: Fibrotic condition; CON: Control group; M1: Model group 1; M2: Model group 2; M3: Model group 3; ***: P<0.001, compared with each other; ****: P<0.000 1, compared with each other; Data were expressed as $\bar{x}\pm s$. ns: No statistical significance.

3 讨 论

阿霉素作为最常用的化疗药物，其心脏毒性涉及诸多病理生理学过程，主要表现为心肌炎、心肌病、急性和慢性充血性心力衰竭[29-33]，及各种心律失常，包括自主神经功能紊乱引起的窦性心动过速[34]、房性期前收缩和心房纤颤[35-36]、房室传导阻滞[37]、室性心律失常[36]，且非持续性室性心动过速较常见[36, 38]。另外，多种信号转导通路、受体参与阿霉素心脏毒性发生发展过程，包括铁代谢障碍和铁死亡[24, 39]、钙超载[40-41]、氧化应激[42-43]、腺苷酸活化蛋白激酶信号转导通路（AMPK signaling pathway）[44]、NRG-1/HER2/Erb B信号转导通路[45-46]、拓扑异构酶2β[47-48]、Toll样受体（Toll-like receptor，TLR）[49-52]、YAP1[53]及P53[54]等。虽然针对阿霉素心脏毒性的基础研究很多，但目前美国食品药品管理局（Food And Drug Administration，FDA）批准应用于临床防治阿霉素心脏毒性的药物仅有右雷佐生（dexrazoxane，DXZ）[55]。然而DXZ也可以抑制作为阿霉素靶点的拓扑异构酶Ⅱ活性，导致阿霉素抗癌效率降低[56]；另外，DXZ显示出致癌潜力，具有发展为急性髓系白血病和骨髓增生异常综合征的风险[57]。因此，阿霉素心脏毒性的机制及干预靶点未来仍需更深入的研究阐明，而公认、统一、稳健的阿霉素诱导的心肌病模型的建立是一切研究的前提。

结合临床评估心脏功能及心脏损伤的常用指标，本实验分别通过小鼠整体情况、心电生理、心脏超声及心脏组织形态学等指标整体评估不同给药方式和剂量造模的优劣。

临床上阿霉素常见的给药方式是通过静脉。动物实验中，给药方式有鼠尾静脉注射、腹腔注射等。静脉注射单次注射药量峰浓度高；腹腔注

射药物吸收缓慢，血药浓度峰浓度相对较低，而阿霉素急性心脏毒性与其峰浓度相关[13]，因此腹腔注射给药安全性高、成模率高。腹腔注射给药其他优势还包括：① 降低了给药难度；② 尾静脉注射易造成鼠尾缺血坏死进而继发感染，而腹腔注射可避免此情况。

临床上心脏超声评估心力衰竭程度、室壁厚度及心室腔内径是金标准，本实验主要结合小鼠心脏超声变化比较造模方式的优劣。本实验结果提示给予阿霉素后QT间期显著延长，这可能是阿霉素引起恶性室性心律失常的基础。临床研究[58]也发现，蒽环类药物治疗与QT间期的改变相关，这与本实验结果相吻合。对使用蒽环类药物治疗的患者发生尖端扭转室速的分析中发现，导致尖端扭转室速最普遍的诱因就是QT间期延长[59]。然而，阿霉素所致QT间期延长的发生机制尚不清楚，有待进一步的研究探索。

临床上常使用心脏标志物评估心力衰竭及心肌损伤程度。临床研究[28]发现，接受阿霉素治疗的儿童心功能不全与正常心功能相比，心功能不全者的血浆NT-pro-BNP 水平显着升高（P＜0.008），所有患者的cTnI水平均低于正常值，这与我们的实验结果一致。因此我们也认为，血浆NT-pro-BNP浓度可能是评估阿霉素心肌病心功能不全有用且敏感的指标。

心肌组织形态学观察可见给予阿霉素后心肌细胞显著空泡化变性，但纤维化病变不显著。既往研究[60]显示，急性损害很少见到纤维化改变，而较长造模周期（持续给药4周，甚至给药结束后第12周处死）中可观察到心肌显著纤维化改变[61]；本实验中未观察到心肌纤维化改变可能的原因是给药时间短，估计短期用药对心肌成纤维细胞影响不大，因此不能观察到心肌纤维化改变；而心肌细胞和心肌肌原纤维的丢失也可能是心肌肌组织排列疏松的原因[62]。病理学检查结果显示，给予阿霉素后心肌细胞径向增大，这与Shen等[63]的研究观测到阿霉素处理后的心肌细胞径向减小相左。然而我们的结果同Wang等[23]的研究观测到阿霉素处理后心肌细胞增大的结果相一致。鉴于目前就阿霉素所致心肌细胞的变化尚存在分歧，因此今后需要开展进一步的实验来阐明心肌细胞形态学变化。

本实验结果显示，阿霉素7.5 mg/kg，隔天给药2次，腹腔注射给药组成模率最高。阿霉素单次15 mg/kg或5 mg/kg，每天1次（连续3 d）给药时，均因为血药浓度峰浓度高，短时间小鼠难以代谢，瞬时药物毒性大，易造成动物死亡。而低于7.5 mg/kg的长时程给药，由于给药间期较长，血药浓度呈周期性变化，不能一直维持有效血药浓度。

腹腔注射阿霉素构建阿霉素诱导的心肌病小鼠模型方法简便、可靠。本研究结果为未来探索阿霉素诱导的心肌病发病机制及干预策略奠定了基础。

利益冲突声明：所有作者均声明不存在利益冲突。

［参　考　文　献］

［1］ WILD C P, WEIDERPASS E, STEWART B W, et al. World cancer report: cancer research for cancer prevention. Lyon, France: International Agency for Research on Cancer［R］, 2020.

［2］ SIEGEL R L, MILLER K D, FUCHS H E, et al. Cancer statistics, 2021［J］. CA A Cancer J Clin, 2021, 71(1): 7-33.

［3］ ZHENG R S, ZHANG S W, ZENG H M, et al. Cancer incidence and mortality in China, 2016［J］. J Natl Cancer Cent, 2022, 2(1): 1-9.

［4］ ARMENIAN S H, LACCHETTI C, BARAC A, et al. Prevention and monitoring of cardiac dysfunction in survivors of adult cancers: American Society of Clinical Oncology clinical practice guideline［J］. J Clin Oncol, 2017, 35(8): 893-911.

［5］ ARMENIAN S H, ROBISON L L. Childhood cancer survivorship: an update on evolving paradigms for understanding pathogenesis and screening for therapy-related late effects［J］. Curr Opin Pediatr, 2013, 25(1): 16-22.

［6］ GUDMUNDSDOTTIR T, WINTHER J F, DE FINE LICHT S, et al. Cardiovascular disease in adult life after childhood cancer in Scandinavia: a population-based cohort study of 32 308 one-year survivors［J］. Int J Cancer, 2015, 137(5): 1176-1186.

［7］ HARVEY V J, SLEVIN M L, PONDER B A, et al. Chemotherapy of diffuse malignant mesothelioma. Phase Ⅱ trials of single-agent 5-fluorouracil and adriamycin［J］. Cancer, 1984, 54(6): 961-964.

［8］ SØRENSEN P G, BACH F, BORK E, et al. Randomized trial of doxorubicin versus cyclophosphamide in diffuse malignant pleural mesothelioma［J］. Cancer Treat Rep, 1985, 69(12): 1431-1432.

[9] SCHERPEREEL A, BERGHMANS T, LAFITTE J J, et al. Valproate-doxorubicin: promising therapy for progressing mesothelioma. A phase Ⅱ study [J]. Eur Respir J, 2011, 37(1): 129-135.
[10] BUIKHUISEN W A, HIDDINGA B I, BAAS P, et al. Second line therapy in malignant pleural mesothelioma: a systematic review [J]. Lung Cancer, 2015, 89(3): 223-231.
[11] DIMARCO A, GAETANI M, OREZZI P, et al. "Daunomycin", a new antibiotic of the rhodomycin group [J]. Nature, 1964, 201: 706-707.
[12] CHABNER B A, LONGO D L. Cancer chemotherapy and biotherapy: principles and practice [M]. Lippincott Williams & Wilkins, 2011.
[13] COUFAL N, FARNAES L. Anthracyclines and anthraceneodiones [M]//Cancer management in man: chemotherapy, biological therapy, hyperthermia and supporting measures. Dordrecht: Springer Netherlands, 2010: 87-102.
[14] CURIGLIANO G, CARDINALE D, SUTER T, et al. Cardiovascular toxicity induced by chemotherapy, targeted agents and radiotherapy: ESMO clinical practice guidelines [J]. Ann Oncol, 2012, 23(Suppl 7): Ⅶ155-166.
[15] ZHANG X, HU C, KONG C Y, et al. FNDC5 alleviates oxidative stress and cardiomyocyte apoptosis in doxorubicin-induced cardiotoxicity via activating AKT [J]. Cell Death Differ, 2020, 27(2): 540-555.
[16] SANGOMLA S, SAIFI M A, KHURANA A, et al. Nanoceria ameliorates doxorubicin induced cardiotoxicity: possible mitigation via reduction of oxidative stress and inflammation [J]. J Trace Elem Med Biol, 2018, 47: 53-62.
[17] RUSSO M, GUIDA F, PAPARO L, et al. The novel butyrate derivative phenylalanine-butyramide protects from doxorubicin-induced cardiotoxicity [J]. Eur J Heart Fail, 2019, 21(4): 519-528.
[18] ZHAO L S, QI Y, XU L N, et al. microRNA-140-5p aggravates doxorubicin-induced cardiotoxicity by promoting myocardial oxidative stress via targeting Nrf2 and Sirt2 [J]. Redox Biol, 2018, 15: 284-296.
[19] ZHANG H W, XU A D, SUN X, et al. Self-maintenance of cardiac resident reparative macrophages attenuates doxorubicin-induced cardiomyopathy through the SR-A1-c-Myc axis [J]. Circ Res, 2020, 127(5): 610-627.
[20] HU C, ZHANG X, WEI W Y, et al. Matrine attenuates oxidative stress and cardiomyocyte apoptosis in doxorubicin-induced cardiotoxicity via maintaining AMPKα/UCP2 pathway [J]. Acta Pharm Sin B, 2019, 9(4): 690-701.
[21] TADOKORO T, IKEDA M, IDE T, et al. Mitochondria-dependent ferroptosis plays a pivotal role in doxorubicin cardiotoxicity [J]. JCI Insight, 2020, 5(9): 132747.
[22] WANG C Y, CHEN C C, LIN M H, et al. TLR9 binding to beclin 1 and mitochondrial SIRT3 by a sodium-glucose co-transporter 2 inhibitor protects the heart from doxorubicin toxicity [J]. Biology (Basel), 2020, 9(11): E369.
[23] WANG A J, TANG Y F, ZHANG J J, et al. Cardiac SIRT1 ameliorates doxorubicin-induced cardiotoxicity by targeting sestrin 2 [J]. Redox Biol, 2022, 52: 102310.
[24] FANG X X, WANG H, HAN D, et al. Ferroptosis as a target for protection against cardiomyopathy [J]. PNAS, 2019, 116(7): 2672-2680.
[25] CHAN B Y H, ROCZKOWSKY A, CHO W J, et al. MMP inhibitors attenuate doxorubicin cardiotoxicity by preventing intracellular and extracellular matrix remodelling [J]. Cardiovasc Res, 2021, 117(1): 188-200.
[26] GUPTA S K, GARG A, BÄR C, et al. Quaking inhibits doxorubicin-mediated cardiotoxicity through regulation of cardiac circular RNA expression [J]. Circ Res, 2018, 122(2): 246-254.
[27] WU X T, WANG L J, WANG K, et al. ADAR2 increases in exercised heart and protects against myocardial infarction and doxorubicin-induced cardiotoxicity [J]. Mol Ther, 2022, 30(1): 400-414.
[28] SOKER M, KERVANCIOGLU M. Plasma concentrations of NT-pro-BNP and cardiac troponin-I in relation to doxorubicin-induced cardiomyopathy and cardiac function in childhood malignancy [J]. Saudi Med J, 2005, 26(8): 1197-1202.
[29] SAWICKI K T, SALA V, PREVER L, et al. Preventing and treating anthracycline cardiotoxicity: new insights [J]. Annu Rev Pharmacol Toxicol, 2021, 61: 309-332.
[30] FERRANS V J. Overview of cardiac pathology in relation to anthracycline cardiotoxicity [J]. Cancer Treat Rep, 1978, 62(6): 955-961.
[31] SHAN K, LINCOFF A M, YOUNG J B. Anthracycline-induced cardiotoxicity [J]. Ann Intern Med, 1996, 125(1): 47-58.
[32] BERRY G J, JORDEN M. Pathology of radiation and anthracycline cardiotoxicity [J]. Pediatr Blood Cancer, 2005, 44(7): 630-637.
[33] SWAIN S M, WHALEY F S, EWER M S. Congestive heart failure in patients treated with doxorubicin: a retrospective analysis of three trials [J]. Cancer, 2003, 97(11): 2869-2879.
[34] JONES L W, HAYKOWSKY M, PEDDLE C J, et al. Cardiovascular risk profile of patients with HER2/neu-positive breast cancer treated with anthracycline-taxane-containing adjuvant chemotherapy and/or trastuzumab [J]. Cancer Epidemiol Biomarkers Prev, 2007, 16(5): 1026-31.
[35] AMIOKA M, SAIRAKU A, OCHI T, et al. Prognostic significance of new-onset atrial fibrillation in patients with non-Hodgkin's lymphoma treated with anthracyclines [J]. Am J Cardiol, 2016, 118(9): 1386-1389.
[36] MAZUR M, WANG F L, HODGE D O, et al. Burden of cardiac arrhythmias in patients with anthracycline-related cardiomyopathy [J]. JACC Clin Electrophysiol, 2017, 3(2): 139-150.
[37] KILICKAP S, BARISTA I, AKGUL E, et al. Early and late arrhythmogenic effects of doxorubicin [J]. South Med J, 2007, 100(3): 262-265.
[38] FRADLEY M G, VIGANEGO F, KIP K, et al. Rates and risk of arrhythmias in cancer survivors with chemotherapy-

induced cardiomyopathy compared with patients with other cardiomyopathies [J]. Open Heart, 2017, 4(2): e000701.

[39] QIN Y, GUO T, WANG Z, et al. The role of iron in doxorubicin-induced cardiotoxicity: recent advances and implication for drug delivery [J]. J Mater Chem B, 2021, 9(24): 4793-4803.

[40] IKEDA S, MATSUSHIMA S, OKABE K, et al. Blockade of L-type Ca2+ channel attenuates doxorubicin-induced cardiomyopathy via suppression of CaMKⅡ-NF-κB pathway [J]. Sci Rep, 2019, 9(1): 9850.

[41] ZHANG Y S, KNIGHT W, CHEN S, et al. Multiprotein complex with TRPC (transient receptor potential-canonical) channel, PDE1C (phosphodiesterase 1C), and A2R (adenosine A2 receptor) plays a critical role in regulating cardiomyocyte cAMP and survival [J]. Circulation, 2018, 138(18): 1988-2002.

[42] HU C, ZHANG X, SONG P, et al. Meteorin-like protein attenuates doxorubicin-induced cardiotoxicity via activating cAMP/PKA/SIRT1 pathway [J]. Redox Biol, 2020, 37: 101747.

[43] PAN J A, ZHANG H, LIN H, et al. Irisin ameliorates doxorubicin-induced cardiac perivascular fibrosis through inhibiting endothelial-to-mesenchymal transition by regulating ROS accumulation and autophagy disorder in endothelial cells [J]. Redox Biol, 2021, 46: 102120.

[44] GRATIA S, KAY L, POTENZA L, et al. Inhibition of AMPK signalling by doxorubicin: at the crossroads of the cardiac responses to energetic, oxidative, and genotoxic stress [J]. Cardiovasc Res, 2012, 95(3): 290-299.

[45] ANJOS M, FONTES-OLIVEIRA M, COSTA V M, et al. An update of the molecular mechanisms underlying doxorubicin plus trastuzumab induced cardiotoxicity [J]. Life Sci, 2021, 280: 119760.

[46] EBRAHIM N, AL SAIHATI H A, MOSTAFA O, et al. Prophylactic evidence of MSCs-derived exosomes in doxorubicin/trastuzumab-induced cardiotoxicity: beyond mechanistic target of NRG-1/erb signaling pathway [J]. Int J Mol Sci, 2022, 23(11): 5967.

[47] MODESTO P N, POLEGATO B F, DOS SANTOS P P, et al. Green tea (camellia sinensis) extract increased topoisomerase Ⅱ β, improved antioxidant defense, and attenuated cardiac remodeling in an acute doxorubicin toxicity model [J]. Oxid Med Cell Longev, 2021, 2021: 8898919.

[48] VEJPONGSA P, YEH E. Topoisomerase 2β: a promising molecular target for primary prevention of anthracycline-induced cardiotoxicity [J]. Clin Pharmacol Ther, 2014, 95(1): 45-52.

[49] BEJI S, D'AGOSTINO M, GAMBINI E, et al. Doxorubicin induces an alarmin-like TLR4-dependent autocrine/paracrine action of nucleophosmin in human cardiac mesenchymal progenitor cells [J]. BMC Biol, 2021, 19(1): 124.

[50] LIU P, BAO H Y, JIN C C, et al. Targeting extracellular heat shock protein 70 ameliorates doxorubicin-induced heart failure through resolution of toll-like receptor 2-mediated myocardial inflammation [J]. J Am Heart Assoc, 2019, 8(20): e012338.

[51] MA Z G, KONG C Y, WU H M, et al. Toll-like receptor 5 deficiency diminishes doxorubicin-induced acute cardiotoxicity in mice [J]. Theranostics, 2020, 10(24): 11013-11025.

[52] SENEVIRATNE A K, XU M J, HENAO J J A, et al. The mitochondrial transacylase, tafazzin, regulates for AML stemness by modulating intracellular levels of phospholipids [J]. Cell Stem Cell, 2019, 24(4): 621-636.e16.

[53] WANG P X, WANG M H, HU Y H, et al. Isorhapontigenin protects against doxorubicin-induced cardiotoxicity via increasing YAP1 expression [J]. Acta Pharm Sin B, 2021, 11(3): 680-693.

[54] XIAO M J, TANG Y F, WANG J (, et al. A new FGF1 variant protects against adriamycin-induced cardiotoxicity via modulating p53 activity [J]. Redox Biol, 2022, 49: 102219.

[55] SHAIKH F, DUPUIS L L, ALEXANDER S, et al. Cardioprotection and second malignant neoplasms associated with dexrazoxane in children receiving anthracycline chemotherapy: a systematic review and meta-analysis [J]. J Natl Cancer Inst, 2016, 108(4): djv357.

[56] JIRKOVSKÁ A, KARABANOVICH G, KUBEŠ J, et al. Structure-activity relationship study of dexrazoxane analogues reveals ICRF-193 as the most potent bisdioxopiperazine against anthracycline toxicity to cardiomyocytes due to its strong topoisomerase Ⅱβ interactions [J]. J Med Chem, 2021, 64(7): 3997-4019.

[57] TEBBI C K, LONDON W B, FRIEDMAN D, et al. Dexrazoxane-associated risk for acute myeloid leukemia/myelodysplastic syndrome and other secondary malignancies in pediatric Hodgkin's disease [J]. J Clin Oncol, 2007, 25(5): 493-500.

[58] HORACEK J M, JAKL M, HORACKOVA J, et al. Assessment of anthracycline-induced cardiotoxicity with electrocardiography [J]. Exp Oncol, 2009, 31(2): 115-117.

[59] ARBEL Y, SWARTZON M, JUSTO D. QT prolongation and Torsades de Pointes in patients previously treated with anthracyclines [J]. Anticancer Drugs, 2007, 18(4): 493-498.

[60] TAKEMURA G, FUJIWARA H. Doxorubicin-induced cardiomyopathy from the cardiotoxic mechanisms to management [J]. Prog Cardiovasc Dis, 2007, 49(5): 330-352.

[61] KUNO A, HOSODA R, TSUKAMOTO M, et al. SIRT1 in the cardiomyocyte counteracts doxorubicin-induced cardiotoxicity via regulating histone H2AX [J]. Cardiovasc Res, 2022: cvac026.

[62] SINGAL P K, ILISKOVIC N. Doxorubicin-induced cardiomyopathy [J]. N Engl J Med, 1998, 339(13): 900-5.

[63] SHEN Y H, ZHANG H, NI Y Y, et al. Tripartite motif 25 ameliorates doxorubicin-induced cardiotoxicity by degrading p85α [J]. Cell Death Dis, 2022, 13(7): 643.

（收稿日期：2022-08-08 修回日期：2022-10-18）